Label-free deep-tissue imaging in vivo using adaptive optical coherence microscopy

Yonghyeon Jo[a,b], Moonseok Kim[a,b], Jin Hee Hong[a,b], Seokchan Yoon[a,b], Pilsung Kang[a,b], Yongwoo Kwon[a,b] Suhyun Kim[c], Hae-Chul Park[c] and Wonshik Choi [a,b,*]

[a] Center for Molecular Spectroscopy and Dynamics, Institute for Basic Science (IBS), Seoul 02841, Republic of Korea
[b] Department of Physics, Korea University, Seoul 02841, Korea
[c] Department of Biomedical Sciences, Korea University, Ansan 15355, Korea
*wonshik@korea.ac.kr

Abstract

Coherent optical imaging has been a useful tool for imaging of living biological subject, but its applicability has been limited to the superficial layers or early developmental stages due to the specimen-induced aberration and multiple light scattering. We propose label-free adaptive optical coherence microscopy free from hardware feedback. Experimental setup is based on wide-field and time-gated interferometric microscopy. Wide-field configuration enables us to collect whole optical modes, thereby offering optimal correction of high-order aberration. Data acquisition is simplified by arithmetic adaptive optical correction by post processing. Owing to improved data acquisition speed, the proposed method is readily applicable for biomedical applications. As a prospective application, we performed label-free neuroimaging of a living zebrafish and visualized tomographic details of neural network.

Motivation

Adaptive optics in microscopy: sensor-based

N. Ji. Nature Method, 14, 374-380 (2017)
W. Zheng, *et al.* Nature Method, 14, 869-872 (2017)

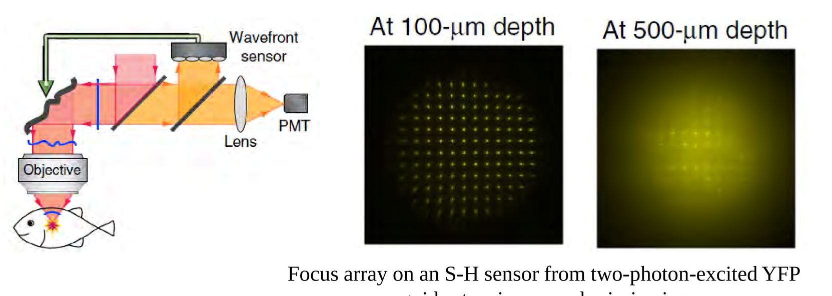

Focus array on an S-H sensor from two-photon-excited YFP guide stars in mouse brain *in vivo*

- Direct wavefront sensing with Shack-Hartmann wavefront sensor or coherence-gated wavefront sensing is fast in acquisition of the aberration map.
- But only works when there are sufficient ballistic, unscattered photons of the guide star.

Adaptive optics in microscopy: sensor-less

N. Ji. Nature Method, 14, 374-380 (2017)
C.Wang, *et al.* Nature Methods, 11, 1037–1040 (2014)

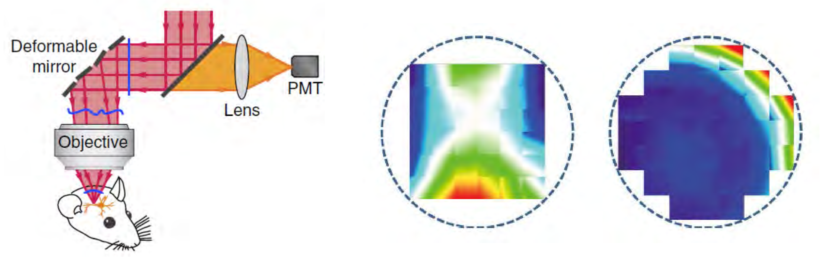

- Indirect wavefront sensing with feedback method can image the structures in deeper depth.
- But the speed is slower than sensor-based method.
- They essentially needs labeling

Imaging method	Advantages	Disadvantages	
Sensor-based	- Fast acquisition of aberration	- Weak at scattering - Cannot separate input/output aberrations	Needs a guide star
Sensor-less	- Can penetrate deeper	- Relatively slow	

Previous study

Light undergoes wavefront distortion - scattering and aberration

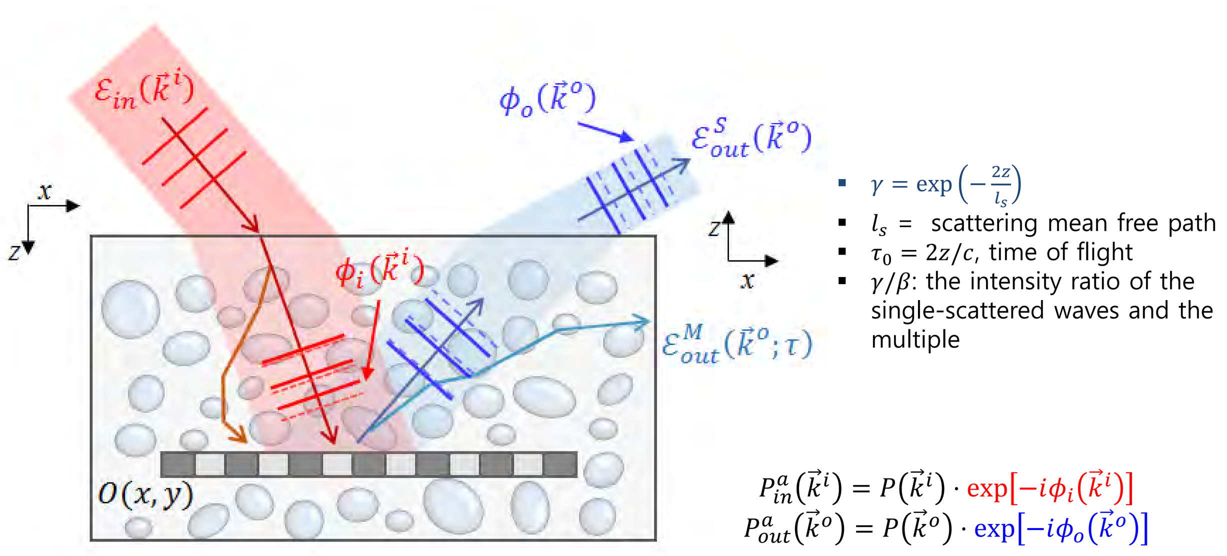

- $\gamma = \exp\left(-\frac{2z}{l_s}\right)$
- l_s = scattering mean free path
- $\tau_0 = 2z/c$, time of flight
- γ/β: the intensity ratio of the single-scattered waves and the multiple

$$P^a_{in}(\vec{k}^i) = P(\vec{k}^i)\cdot\exp[-i\phi_i(\vec{k}^i)]$$
$$P^a_{out}(\vec{k}^o) = P(\vec{k}^o)\cdot\exp[-i\phi_o(\vec{k}^o)]$$

$$\mathcal{E}(\vec{k}^o;\vec{k}^i,\tau_0) = \sqrt{\gamma}\mathcal{E}^S_{out}(\vec{k}^i+\Delta\vec{k};\tau_0) + \sqrt{\beta}\mathcal{E}^M_{out}(\vec{k}^i+\Delta\vec{k};\tau_0)$$
$$= \sqrt{\gamma}\,P^a_{out}(\vec{k}^i+\Delta\vec{k})O(\Delta\vec{k})P^a_{in}(\vec{k}^i) + \sqrt{\beta}\mathcal{E}^M_{out}(\vec{k}^i+\Delta\vec{k};\tau_0)$$

$$\mathcal{E}_{Coherent}(\Delta\vec{k}) = \sum_{\vec{k}^o-\vec{k}^i=\Delta\vec{k}} \mathcal{E}_o(\vec{k}^o=\vec{k}^i+\Delta\vec{k}) = \sqrt{\gamma}O(\Delta\vec{k})\cdot\sum_{\vec{k}^i}P^a_{in}(\vec{k}^i)P^a_o(\vec{k}^i+\Delta\vec{k}) + \sqrt{\beta}\sum_{\vec{k}^i}\mathcal{E}^M_o(\vec{k}^i+\Delta\vec{k})$$

$$\left|\sum_{\vec{k}^i}P^a_i(\vec{k}^i)P^a_o(\vec{k}^i+\Delta\vec{k})\right| \le \left|\sum_{\vec{k}^i}P(\vec{k}^i)P(\vec{k}^i+\Delta\vec{k})\right| \Rightarrow \left|\sum_{\vec{k}^i}P^a_{in}(\vec{k}^i)P^a_{out}(\vec{k}^i+\Delta\vec{k})\right| \approx \left|\sum_{\vec{k}^i}P(\vec{k}^i)P(\vec{k}^i+\Delta\vec{k})\right|$$

- The cross-correlation between the complex pupil functions amplifies the object function in proportion to the number of incident wave vectors.

Time-resolved reflection matrix imaging - Collective Accumulation of Single-Scattered wave (CASS)

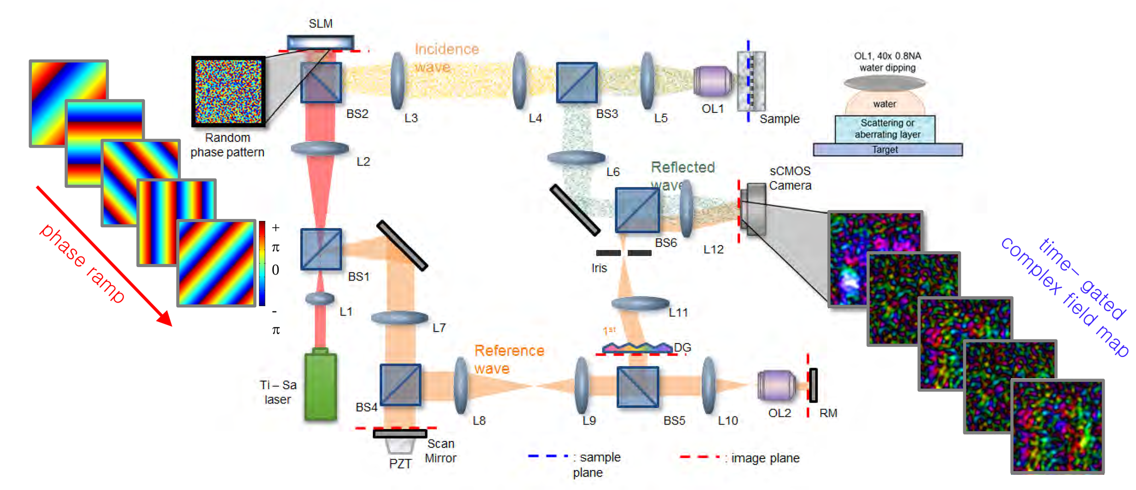

- Source : mode-locked Ti-Sapphire laser (center wavelength 800nm, bandwidth 30nm, and pulse width 100fs)
- Wide-field detection by interference microscope
- Resolution ~ 0.6 μm (lateral, diffraction limited), coherence length : 15 μm

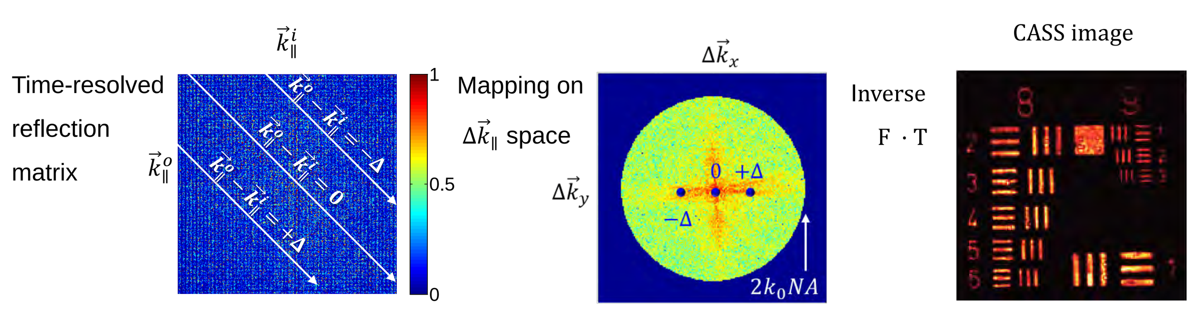

S. Kang, S. Jeong *et al*, Nature photonics **9**, 253-258 (2015)

Previous study

Aberration correction(1) : forward process

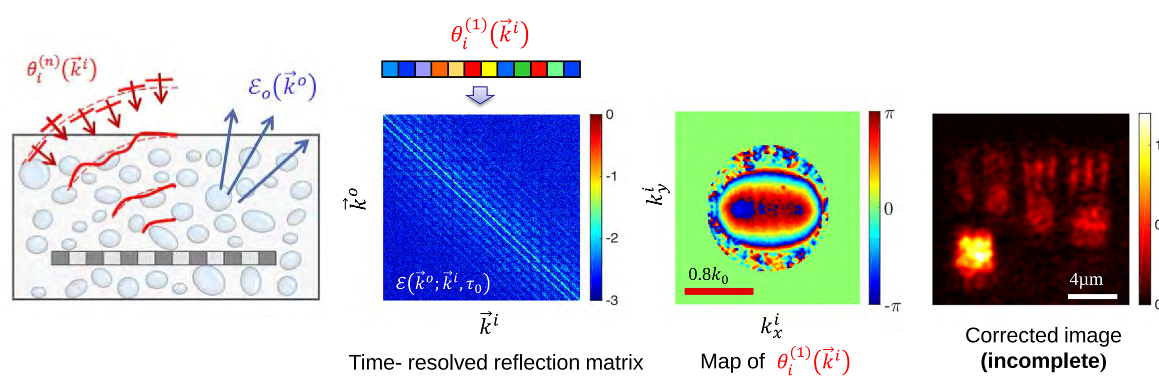

$$\mathcal{E}^{(1)}_{CLASS}(\Delta\vec{k}) = \sum_{\vec{k}^i}\mathcal{E}(\vec{k}^i+\Delta\vec{k};\vec{k}^i)\,e^{i\theta_i^{(1)}(\vec{k}^i)}$$
$$= \sqrt{\gamma}O(\Delta\vec{k})\cdot\Sigma_{\vec{k}^i}P^a_o(\vec{k}^i+\Delta\vec{k})P^a_i(\vec{k}^i)e^{i\theta_i^{(1)}(\vec{k}^i)} + \sqrt{\beta}\,\Sigma_{\vec{k}^i}\mathcal{E}^M_o(\vec{k}^i+\Delta\vec{k})e^{i\theta_i^{(1)}(\vec{k}^i)}$$

Aberration correction(2) : phase-conjugation process

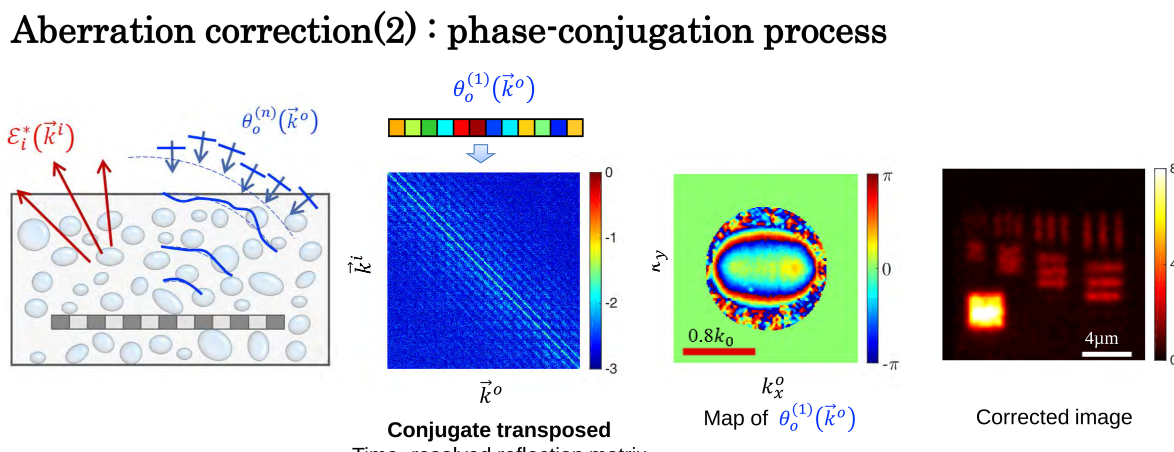

$$\mathcal{E}^{pc}_{CLASS}(\Delta\vec{k}) = \sqrt{\gamma}O^{-1}(\Delta\vec{k})\cdot\sum_{\vec{k}^o}e^{i\theta_i^{(1)}(\vec{k}^i)}P^a_i(\vec{k}^o-\Delta\vec{k})^*P^a_o(\vec{k}^o)^*e^{i\theta_o^{(1)}(\vec{k}^o)}$$
$$+\sqrt{\beta}\sum_{\vec{k}^o}\mathcal{E}^M_o(\vec{k}^i+\Delta\vec{k})^*e^{i\theta_i^{(1)}(\vec{k}^i)+i\theta_o^{(1)}(\vec{k}^o)}$$

Closed-Loop Accumulation of Single-Scattered wave (CLASS)

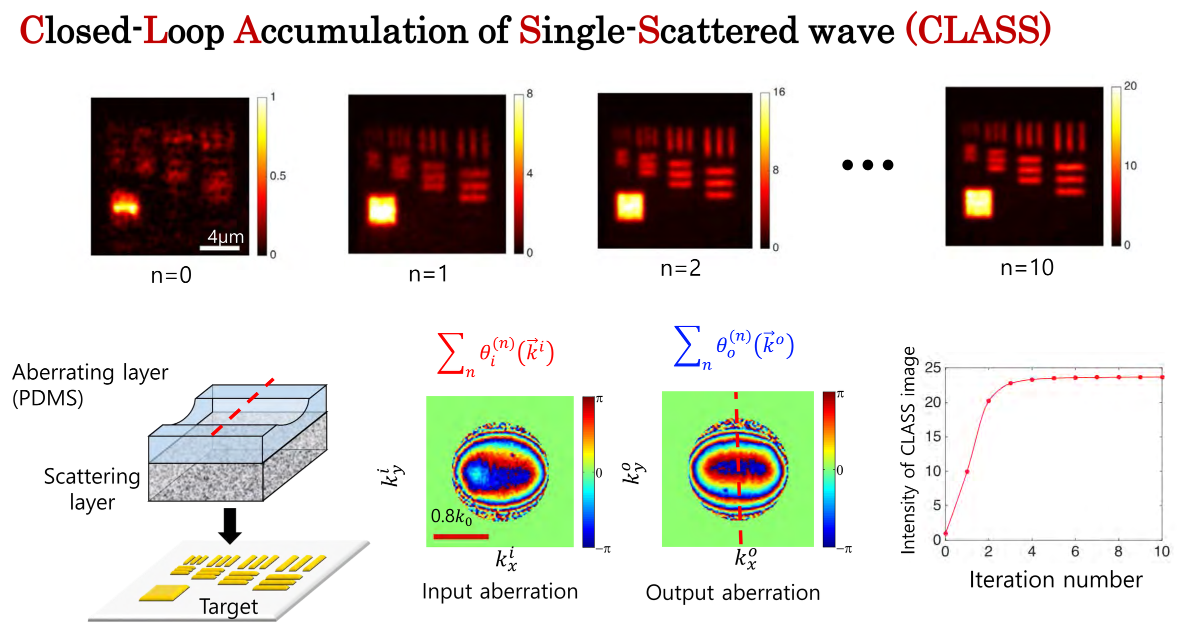

S. Kang, *et al*, Nature Communications, **8**, 2157 (2017)

However, *in vivo* imaging has remained unrealistic thus far because a slow liquid-crystal spatial light modulator should be used for the recording of the reflection matrix

Experimental setup

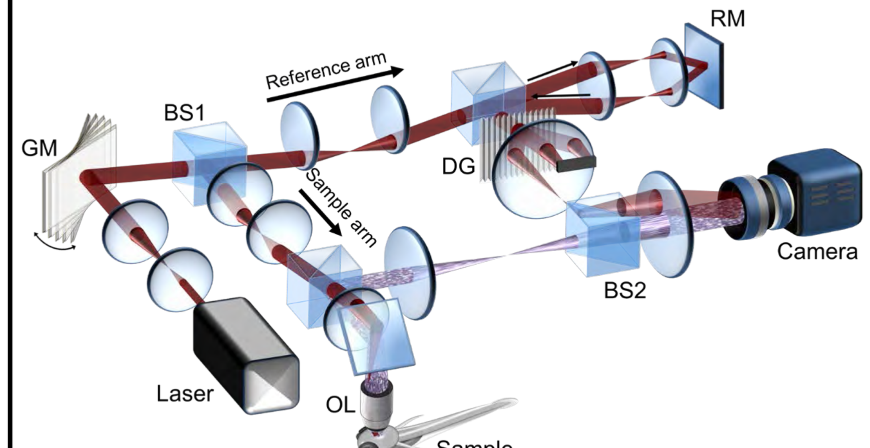

- Source : supercontinuum laser (tunable between 450~750 nm, center wavelength 515 nm)
- Wide-field detection by interference microscope
- NA : 0.8 resolution ~ 0.4 μm (lateral, diffraction limited), coherence length : 10~30 μm
- An anesthetized zebrafish larva at 21 days post-fertilization (dpf)

Effect of the fixed reference

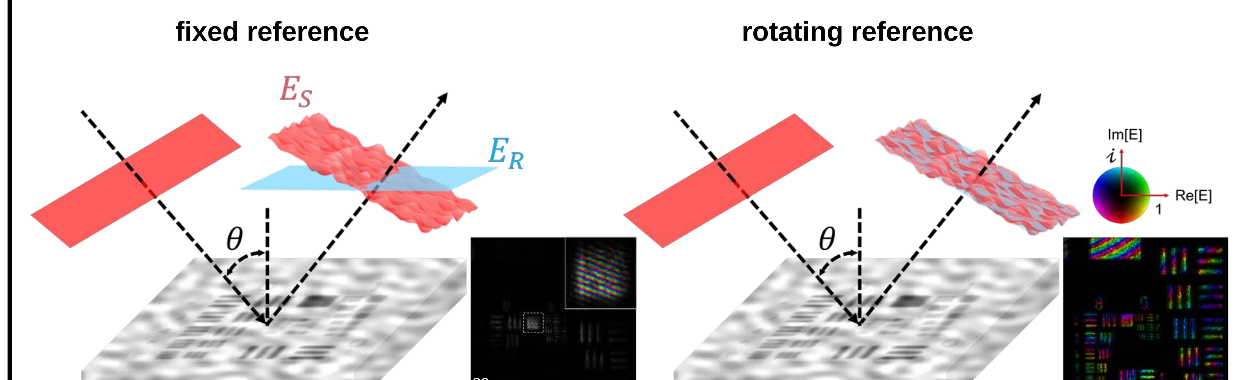

- If the pulse front of the reference wave is fixed and parallel to the camera plane, the interference between sample and reference waves occur only within a narrow range set by the coherence length of light source.

Experimental result

Image processing

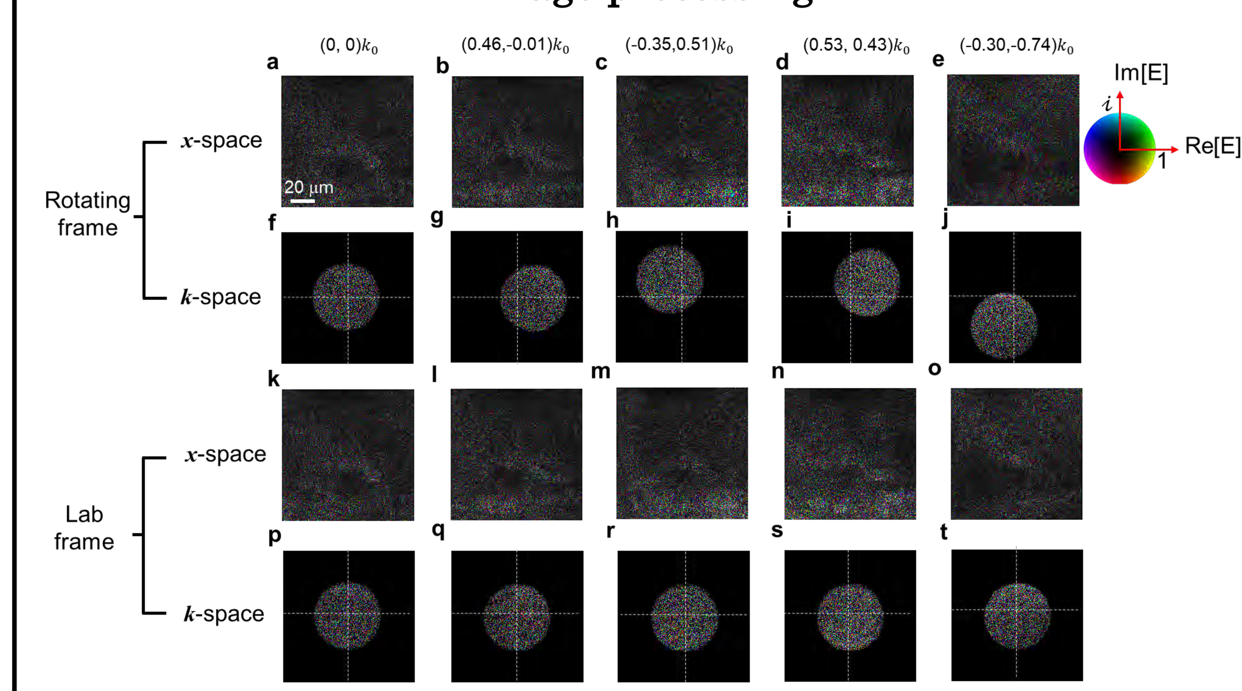

- Raw complex field maps of backscattered waves were measured with respect to the rotating reference wave, and they need to be converted to the maps in the laboratory frame for the application of aberration correction algorithm

Application of CLASS algorithm

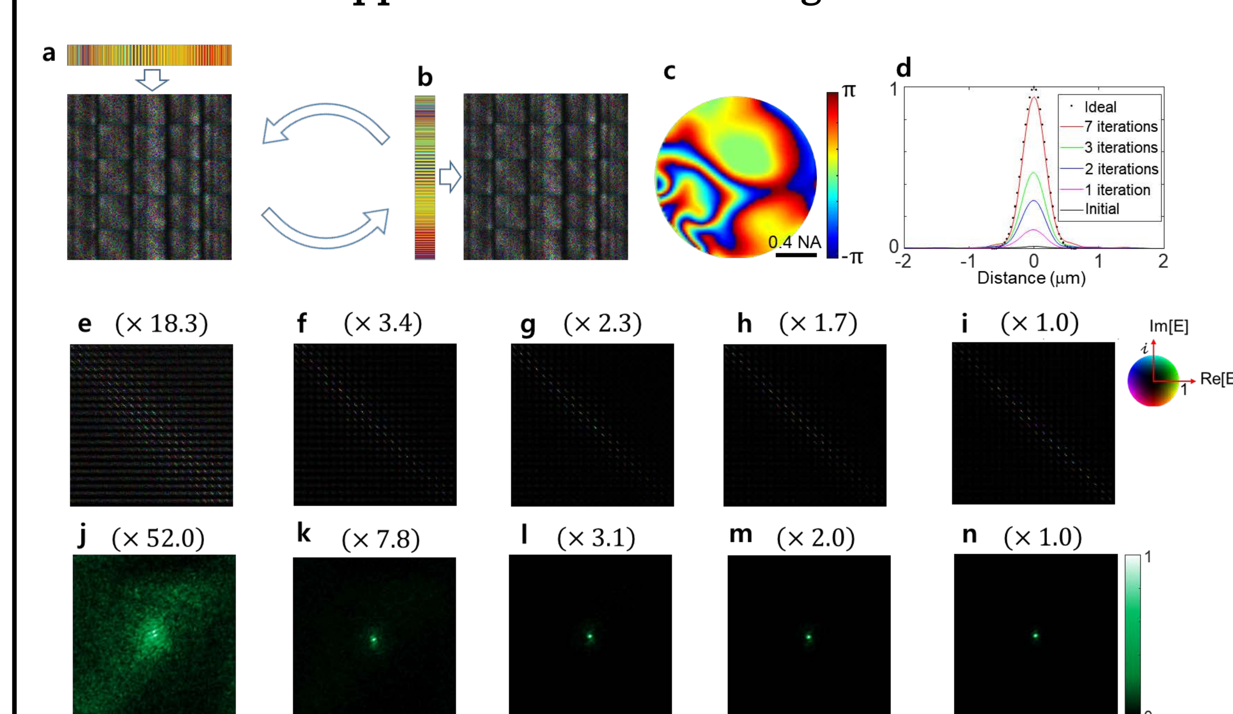

- As the iteration number of the CLASS algorithm increases, time-resolved reflection matrix and point spread function become sharper
- The line profile of the PSF after 7 rounds of iterations (figure d) agrees well with the theoretical prediction (black dots). The absolute value of Strehl ratio was 0.94, confirming that the PSF reaches almost the diffraction-limit spot.
- Strehl ratio enhancement was 52.

Local aberration correction

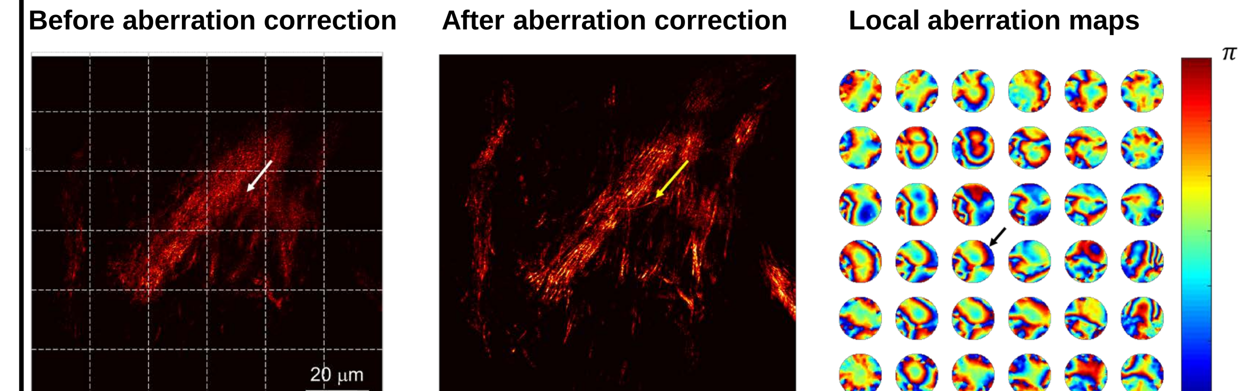

- A 21-dpf zebrafish was placed under the objective lens at an upright position after being anesthetized, and the area close to the ear in the hindbrain was investigated
- The dark area in the yellow dashed box is due to the pigmented scales at the skin
- The white dotted boxes show segmented areas where aberration correction was individually applied
- After aberration correction, the fine filament structures of individual myelinated axons are clearly resolved over the entire field of view. In some areas, such as the one indicated by a yellow arrow, even the fine neuronal processes that used to be invisible before aberration correction appeared
- The aberration maps which differ significantly from one another indicates the spatial variability and complexity of the sample-induced aberrations